Electronic Supplementary Material (ESI) for Physical Chemistry Chemical Physics.

Supplementary Information: Electrochemical phase transformation accompanied with Mg extraction and insertion in spinel $MgMn_2O_4$ cathode material

Takuya Hatakeyama,[1] Norihiko L. Okamoto,[1] Kohei Shimokawa,[1] Hongyi Li,[1] Aiko Nakao,[2] Yoshiharu Uchimoto,[3] Hiroshi Tanimura,[1] Tomoya Kawaguchi,[1] and Tetsu Ichitsubo[1]

[1] *Institute for Materials Research, Tohoku University, Sendai, 980-8577, Japan*
[2] *The Institute of Physical and Chemical Research (RIKEN), Saitama, 351-01, Japan*
[3] *Graduate School of Human and Environmental Studies, Kyoto University, Kyoto 606-8501, Japan*

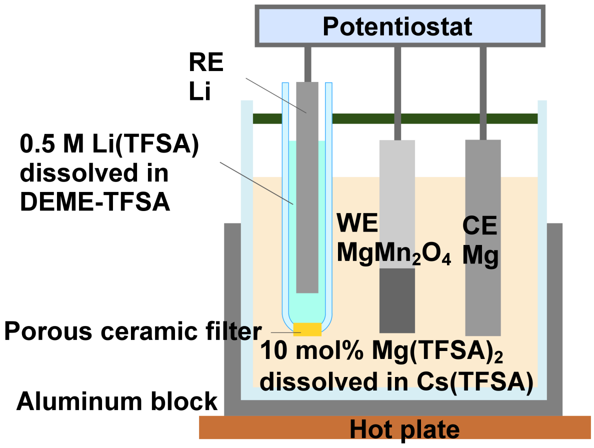

Fig. S1: Schematic illustration of a three-electrode beaker cell used for electrochemical measurements. The Li reference electrode is separated from a $Mg(TFSA)_2$-90 mol% CsTFSA electrolyte using a quartz tube with a porous ceramic part (LiRE). The electrolyte temperature was maintained at 150 °C.

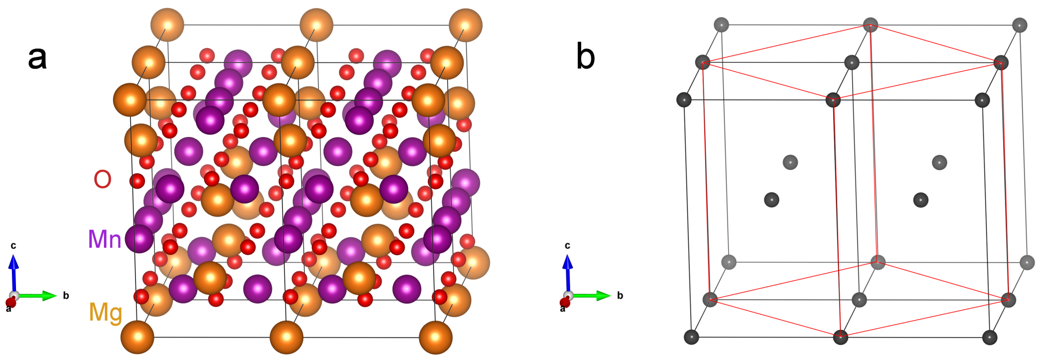

Fig. S2: (a) Crystal structure of tetragonal spinel $MgMn_2O_4$ (Space group: $I4_1/amd$). Wyckoff positions of $4a$, $8d$ and $16h$ are occupied by Mg, Mn and O, respectively. Four I-centered tetragonal lattices are displayed. (b) Relationship between I-centered tetragonal lattices (black lines) and F-centered tetragonal lattices (red lines). Black spheres denote lattice points. In order to simplify the comparison between tetragonal spinels (Space group: $I4_1/amd$) and cubic spinels (Space group: $Fd\text{-}3m$), crystallographic nontation (lattice constant, orientation, etc.) for tetragonal spinels is adopted based on the unconventional F-centered lattice.

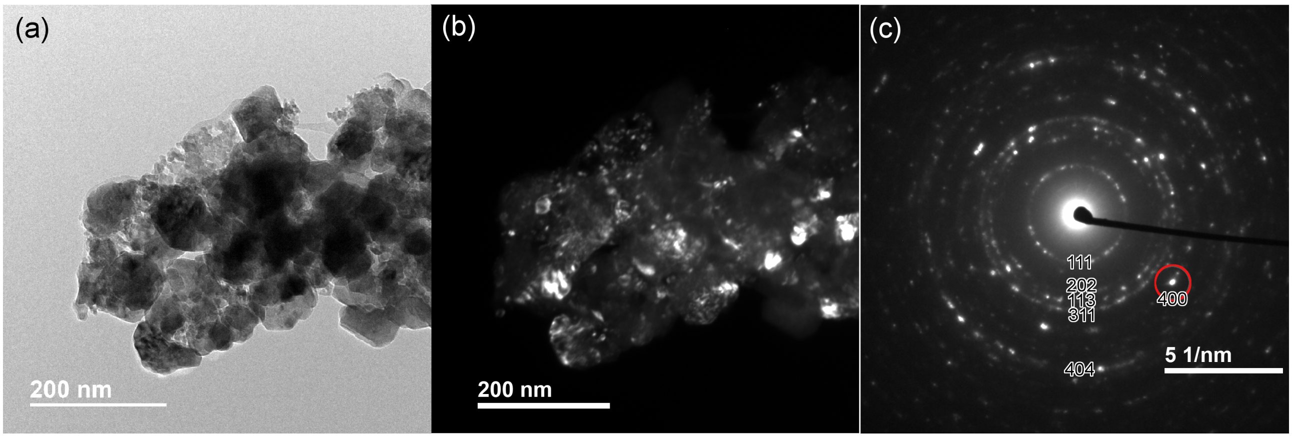

Fig. S3: TEM observation of $MgMn_2O_4$ calcined at 425 °C. (a) Bright field image. (b) dark field image. (c) Selected area diffraction pattern. Dark field image was obtained from a 400 reflection spot circled by red line in the diffraction pattern.

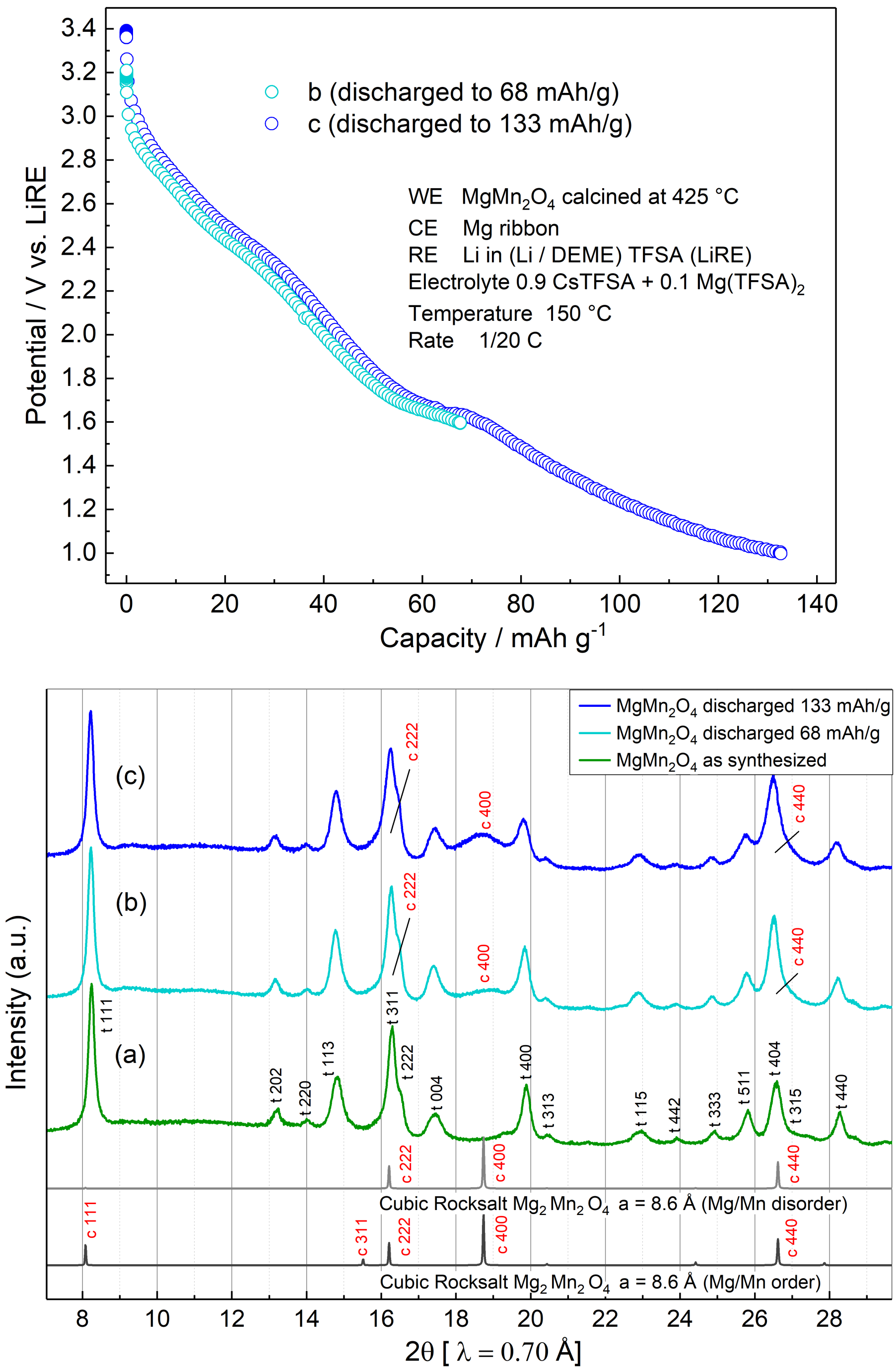

Fig. S4: Mg intercalation into spinel $MgMn_2O_4$. (Top) Discharge profile of $MgMn_2O_4$ starting from as-synthesized state. (Bottom) XRD patterns of $MgMn_2O_4$ discharged from as-synthesized state.

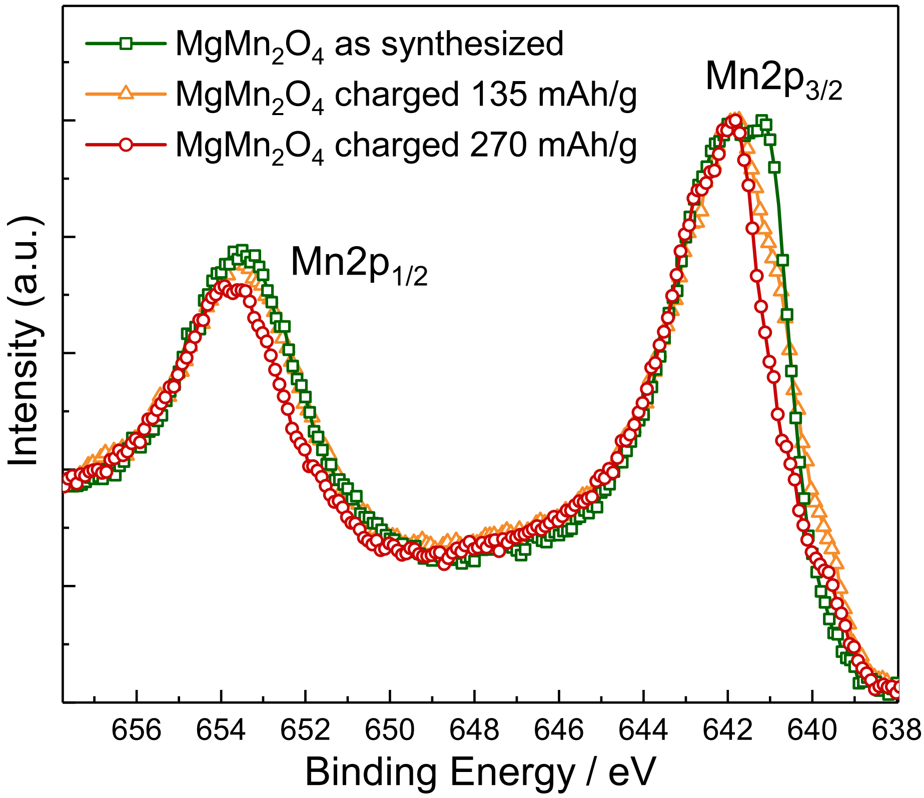

Fig. S5: Mn 2p XPS spectra of pristine and charged $MgMn_2O_4$. The electrodes were galvanostatically charged at a rate of C/20 at 150 °C. Note that the electric charge of 135 and 270 mAh/g involves electrolyte decomposition as well as Mg-deintercalation.

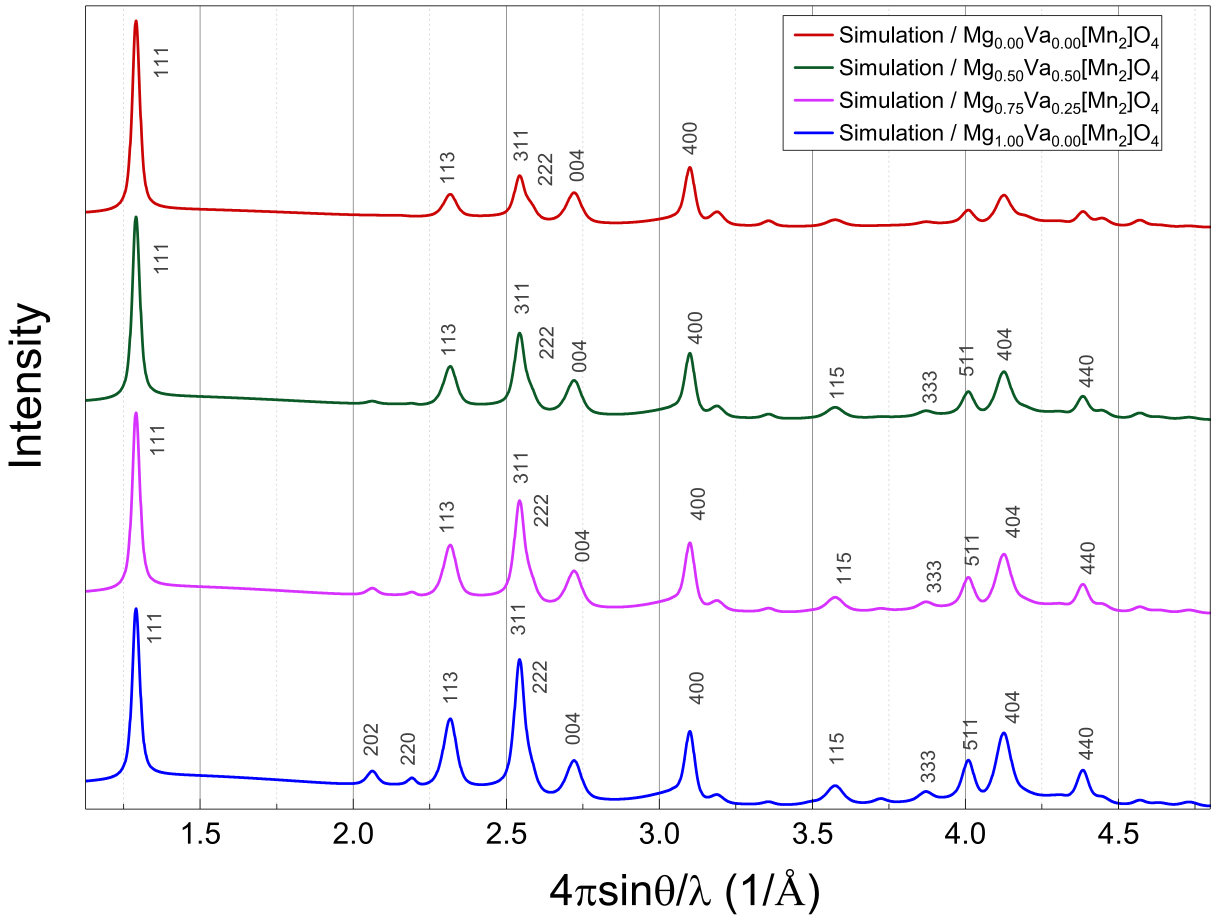

Fig. S6: XRD simulation of tetragonal spinel $Mg_xVa_{1-x}Mn_2O_4$ (Va : vacancy). The simulation is based on non-inverted configuration. Mg-extraction does not significantly change intensity ratios of 113/311, 004/400, and 404/440 diffraction peaks.

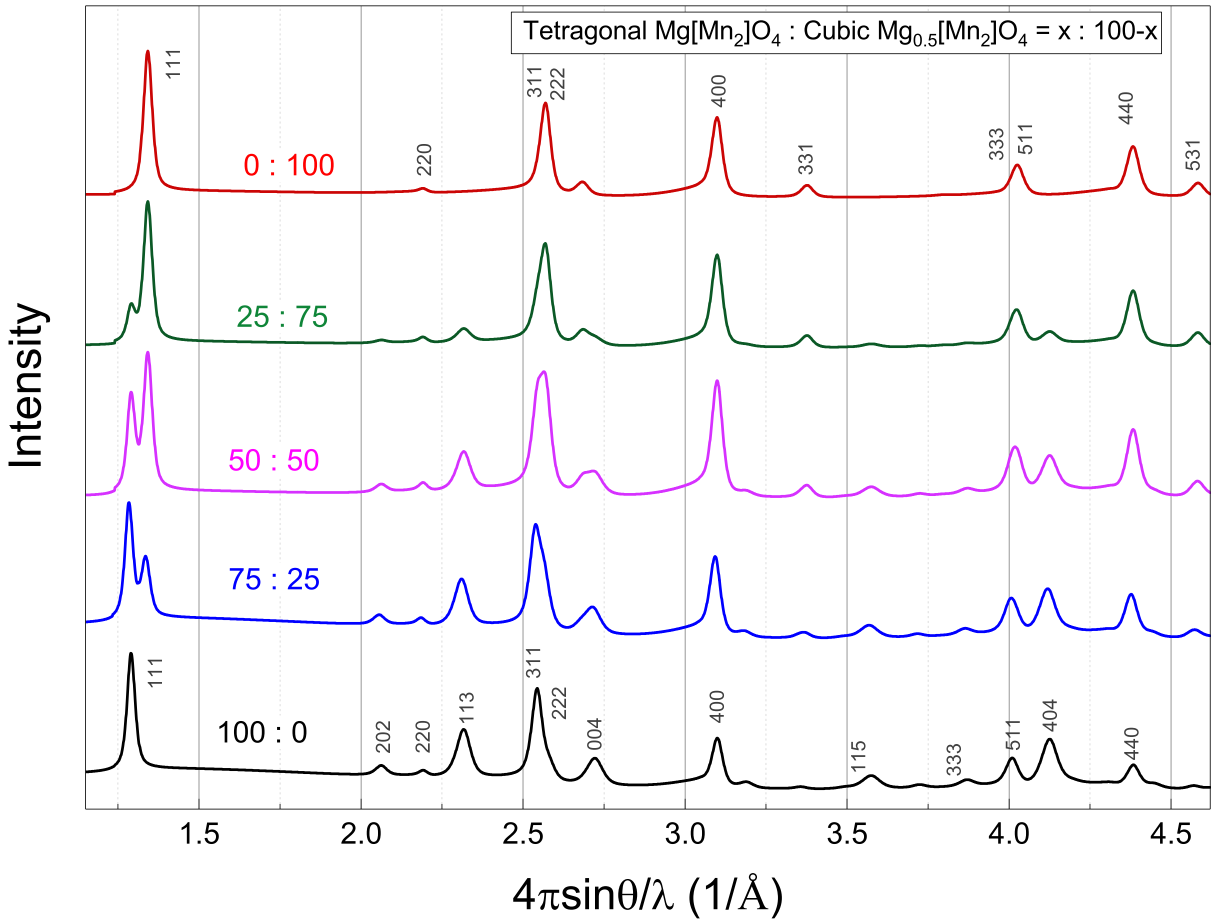

Fig. S7: XRD simulation of cubic spinel $Mg_{0.5}Mn_2O_4$ and tetragonal spinel $MgMn_2O_4$ with different phase ratios. The simulation is based on non-inverted configuration in both cubic $Mg_{0.5}Mn_2O_4$ and tetragonal $MgMn_2O_4$.

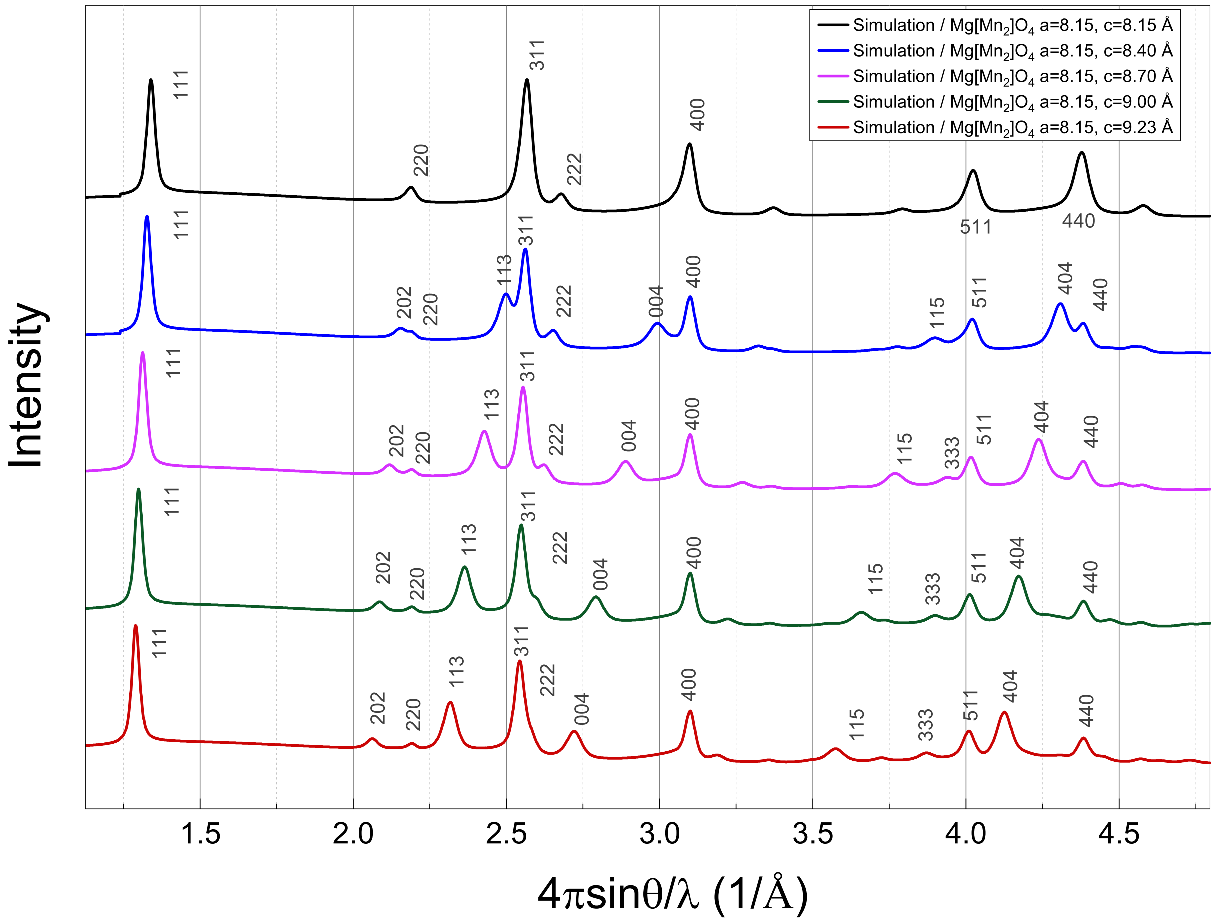

Fig. S8: XRD simulation of tetragonal spinel $MgMn_2O_4$ with different lattice constant c. Lattice shrinkage along c axic converges 113/311, 004/400, and 404/440 diffraction peaks into one peak.

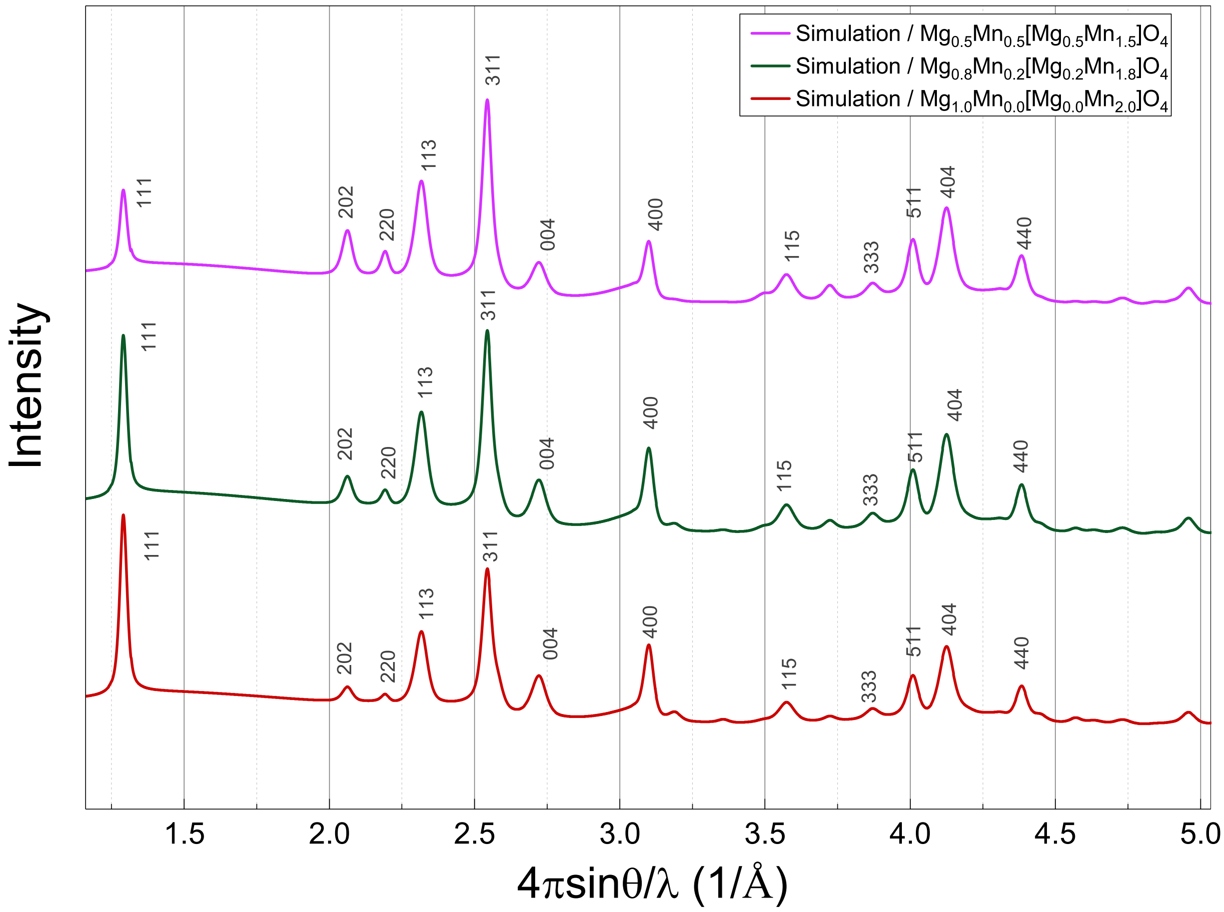

Fig. S9: XRD simulation of inverted configuration in tetragonal spinel $MgMn_2O_4$. with different lattice constant c. Lattice shrinkage along c axic converges 113/311, 004/400, and 404/440 diffraction peaks into one peak.